UC Irvine
UC Irvine Previously Published Works

Title

Proton Block and Voltage Gating Are Potassium-dependent in the Cardiac Leak Channel Kcnk3*

Permalink

Journal

ISSN

Authors

Lopes, Coeli MB
Gallagher, Patrick G
Buck, Marianne E
et al.

Publication Date

DOI

Copyright Information

Peer reviewed

Proton Block and Voltage Gating Are Potassium-dependent in the Cardiac Leak Channel Kcnk3*

Coeli M. B. Lopes, Patrick G. Gallagher‡, Marianne E. Buck, Margaret H. Butler, and Steve A. N. Goldstein§

From the Section of Developmental Biology and Biophysics, Departments of Pediatrics and Cellular and Molecular Physiology, Boyer Center for Molecular Medicine, Yale University School of Medicine, New Haven, Connecticut 06536

Potassium leak conductances were recently revealed to exist as independent molecular entities. Here, the genomic structure, cardiac localization, and biophysical properties of a murine example are considered. Kcnk3 subunits have two pore-forming P domains and unique functional attributes. At steady state, Kcnk3 channels behave like open, potassium-selective, transmembrane holes that are inhibited by physiological levels of proton. With voltage steps, Kcnk3 channels open and close in two phases, one appears to be immediate and one is time-dependent ($\tau = \sim 5$ ms). Both proton block and gating are potassium-sensitive; this produces an anomalous increase in outward flux as external potassium levels rise because of decreased proton block. Single Kcnk3 channels open across the physiological voltage range; hence they are "leak" conductances; however, they open only briefly and rarely even after exposure to agents that activate other potassium channels.

Leak currents are considered essential to normal electrical function in sympathetic ganglia (1, 2), myelinated axons (3–6), carotid body type 1 cells (7), and cardiac myocytes (8–12). Nonetheless, their existence as independent transport entities, rather than residual flux through other pathways, was controversial until the cloning of KCNKØ from *Drosophila melanogaster* (13). KCNKØ (previously ORK1), encodes a potassium channel subunit with two P domains and four predicted transmembrane segments (2P/4TM)[1] (13). KCNKØ channels are open across the physiological voltage range, show no delay in current development with voltage steps, and "openly rectify," that is, they operate like potassium-selective holes in an electric field (13).[2] KCNKØ channels are tightly regulated; activation yields an open probability (P_o) close to 1, and inhibition produces channels that are almost always closed (63).[3] Mam-

malian genes homologous to KCNKØ, now enumerated *KCNK1–9*, are emerging rapidly. Like KCNKØ, those that show function are potassium-selective leak conductances (16–24).

Based on homology to KCNKØ we isolated *Kcnk3* from a murine cardiac cDNA library (16, 24), localized it to chromosome 5B in mouse and 2p23.3-p24.1 in human (25), and called the predicted protein product OAT1. Two other groups cloned *Kcnk3* concurrently and called the encoded subunit TASK1 (26) and TBAK1 (27). For clarity, we will now employ the Human Genome Organization nomenclature: *KCNK3* gene and KCNK3 channel for human isolates and *Kcnk3* and Kcnk3 for mice. Significant discrepancies exist between the findings of the three groups. Although all agree that *Kcnk3* predicts 2P/4TM subunits that form pH-sensitive, openly rectifying potassium channels, there is no consensus as to tissue distribution (atria or ventricle), function (instantaneous or time-dependent, low or high open probability), or the predicted protein sequence.

In this report, five points are highlighted. First, the genomic sequence for murine *Kcnk3* is determined to confirm the accuracy of the cDNA under study; this reveals an intron in the midst of the coding sequence for the signature motif (G YG) of the first P loop (an arrangement seen to be conserved in the family from nematodes to humans). Second, *Kcnk3* messenger RNA is localized to murine cardiac ventricle and, at lower levels, in the atria; Kcnk3 protein is then confirmed to have the same cardiac distribution. Third, half-maximal blockade of Kcnk3 channels by external protons is confirmed to be near physiological pH and shown to be sensitive to external potassium. Fourth, Kcnk3 currents are seen to develop with voltage changes in two phases; one appears to be immediate and one is time-dependent; the fraction of current in each phase is responsive to external potassium. Fifth, single Kcnk3 channels are shown to open only briefly (to one of two conductance levels) and rarely; although open probability increases with depolarization, it is not significantly augmented by a wide array of stimuli including activation or inhibition of protein kinase A or C, application of volatile anesthetics or metabolic poisons, changes in osmotic strength, or exposure to low oxygen tension.

Based on its location and similar functional attributes, we hypothesize Kcnk3 to be the correlate of a native cardiac current that remains active throughout the action potential plateau but whose molecular basis has been unclear, I_{Kp} or I_{Ksus} (8–12, 28). The findings support the idea that Kcnk3 channels link cardiac excitability to changes in acid-base status.

MATERIALS AND METHODS
Cloning of Kcnk3

cDNA—A homology search of NCBI data base using the BLAST program suite (29) and the coding sequence of the ORK1 channel

[1] The abbreviations used are: 2P/4TM, two P domains and four predicted transmembrane segments; bp, base pair(s); kb, kilobase(s); MES, 4-morpholineethanesulfonic acid; PMA, phorbol 12-myristate 13-acetate.

[2] N. Ilan and S. A. N. Goldstein, submitted for publication.

[3] N. Zilberberg, N. Ilan, R. Gonzalez-Colaso, and S. A. N. Goldstein, submitted for publication.

(KCNKØ) as query (accession number U55321) identified expressed sequence tag W09160. Northern blot analysis using the 801-bp cDNA fragment in W09160 detected an abundant single message at ~3.8 kb in murine heart (24). The 801-bp cDNA fragment was used to screen a random primed and oligo(dT)-primed murine heart cDNA library in λγt11 (CLONTECH, Palo Alto, CA). Of 28 clones that hybridized to the probe, eight were purified and subcloned, and their ends subjected to automated DNA sequencing; three clones were sequenced in their entirety. This yielded a 5′-untranslated sequence, an open reading frame, and a 3′-untranslated sequence. An additional 160 bp of the upstream 5′-untranslated sequence was obtained by 5′ rapid amplification of cDNA ends using 1 μg of total RNA prepared from murine cardiac muscle, as described (30) and primer A (5′-CACCAGCAGGTAGGT-GAAG-3′). Single-stranded ligation and amplification were carried out with primers D (5′-GCCAAGCTTGCGGTGGCCCTCAGGTCCAGCTC-3′) with B (5′-GCCGCCGCTGCTGCCCCGGA-3′) and D with C (5′-CTCCACGCCGGGCACCAGCTCCGCAC-3′), respectively. Analyses of nucleotide and predicted amino acid sequences were performed utilizing GCG software from the University of Wisconsin (Madison, WI). The cDNA sequence is listed (accession number AB008537). The coding sequence was placed between the 5′- and 3′-untranslated regions the of *Xenopus* β-globin gene in pBF2 (a gift of Bernd Fakler, Tuebingen, DE) and cRNA produced using T3 RNA polymerase and a kit (Ambion, Austin, TX). Transcripts were quantified by spectrophotometer and compared with control samples separated by agarose gel electrophoresis. Our cDNA sequence (accession number AF065162) was verified by comparison with the genomic sequence (accession numbers AF241798 and AF242508) and varies from the partial sequence reported for murine TASK1 at amino acid residues 4 (Gln replaces Glu), 123 (Val replaces Ile), and 286 (where an additional Gly is added) (26) and murine TBAK1, which includes a 9-residue amino-terminal extension and a single residue difference at position 101 (Pro replaces Ala) (27). These differences do not coincide with known consensus sites in the *Kcnk3* genomic clone (see below) for splice junctions or editing and are judged to be errors in the sequences reported by others.

Genomic—A murine genomic DNA library in bacteriophage P1 was screened with two oligonucleotide primers corresponding to the 3′ end of the coding region of *Kcnk3* cDNA as described (31). These primers, 5′-GCAGACGCAGCCGCAGTATG-3′ and 5′-GCCTGGCCGTTGTGCG-TGAGCAGGG-3′, amplify a 168-bp fragment from murine genomic DNA. Polymerase chain reaction-positive clones were purified and subcloned into pGEM-7Z plasmid vectors (Promega Corp., Madison, WI). Subcloned fragments were analyzed by restriction endonuclease digestion, Southern blotting, and nucleotide sequencing.

Northern Blot and in Situ Hybridization Analyses

[32]P[ATP]-labeled probes used for Northern blots were the 801-bp fragment (W09160) and a β-actin cDNA (Amersham Pharmacia Biotech) (32). *In situ* hybridization was performed with adult C57BL6 mice (Jackson Labs, Bar Harbor, ME) using sense and antisense probes from the 801-bp *Kcnk3* fragment, as described (33). [α-^{35}S]UTP (Amersham Pharmacia Biotech) incorporation into the 801-bp *Kcnk3* fragment was 70–85%. Heart sections (8 μm) were hybridized overnight, treated with ribonuclease-A, and dehydrated by soaking in 100% EtOH in 0.6 M ammonium acetate. Emulsion radiographs were generated by dipping slides in photographic emulsion with development and fixation 2 days later. Slides were placed on Kodak SB5 film to generate images.

Western Blot Analyses

Rabbit antibodies recognizing residues 252–269 of the human KCNK3 subunit, EDEKRDAEHRALLTRNGQ, were purchased from Alamone (APC024, Jerusalem, Israel). Frozen mouse heart ventricle and atria were purchased (Pel-Freez Biologicals, Rogers, AZ), and crude membrane fractions of each tissue were prepared by a modified method (34). Proteins were extracted with 1% Triton X-100 and analyzed by SDS-polyacrylamide gel electrophoresis and Western blot with the rabbit antibody, followed by goat anti-rabbit horseradish peroxidase-conjugated antibody and visualization by enhanced chemiluminescent substrate.

Electrophysiology

Oocytes were isolated from *Xenopus laevis* frogs (Nasco, Atkinson, WI), subjected to collagenase treatment to ease removal of the follicle, and injected with 46 nl of sterile water containing 2–4 ng of *Kcnk3* cRNA.

Whole Cell—Macroscopic currents were measured 1–4 days after cRNA injection by two-electrode voltage clamp using a Geneclamp 500 amplifier (Axon Instruments, Foster City, CA). Data were sampled at 4–20 kHz and filtered at 1–5 kHz. Data acquisition and analysis were performed using Pulse (Instrutech, Great Neck, NY) and Sigmaplot (Jandel Scientific, San Rafael, CA) software. Electrodes were made from 1.5-mm borosilicate glass tubes (Garner Glass Co., Claremont, CA), contained 3 M KCl, and had resistances between 0.3 and 1 MΩ. Oocytes were studied while perfused at 0.5–1 ml/min with 5 mM KCl bath solution 93 mM NaCl, 5 mM KCl, 1 mM MgCl$_2$, 0.3 mM CaCl$_2$, 5 mM HEPES, pH 7.4, with NaOH. In indicated cases, KCl was substituted for NaCl. For solutions at pH 6.0, MES replaced HEPES. Studies were performed at room temperature.

Membrane Patch—Voltage clamp recordings were made in both on-cell and outside-out configuration using an Axopatch 200A amplifier (Axon Instruments). The vitelline layer was removed prior to recording with a pair of fine forceps after a 1–2-min incubation in hypertonic solution 200 mM KCl and potassium aspartate, 20 mM KCl, 1 mM MgCl$_2$, 10 mM EGTA, 10 mM HEPES, pH 7.4, with NaOH. Pipettes were fabricated from 7052 glass (Garner Glass Co., Claremont, CA) coated with Q-Dope (GC Electronics, Rockford, IL) and fire-polished. The electrode solution for outside-out patches was 100 mM KCl, 5 mM EGTA, 1 mM MgCl$_2$, 5 mM HEPES, pH 7.4, with KOH. Bath solution contained 100 mM KCl, 0.3 mM CaCl$_2$, 1 mM MgCl$_2$, 5 mM HEPES, pH 7.4. External potassium concentration was varied by substitution of NaCl for KCl. Pipette resistance ranged from 3–5 MΩ for single channel recordings and 0.3–0.6 MΩ for macropatches; seal resistance was 4–15 GΩ. Data were sampled at 10–40 kHz, filtered at 0.5–5 kHz with ACQUIRE software (Instrutech Corp.), and analyzed off-line by TAC (Instrutech Corp.) and IGOR (Wavemetrics, Lake Oswego, OR) software.

Calculations—Equilibrium reversal potentials were determined in the indicated solutions by linear regression. Current-voltage relations were studied in various potassium solutions and fit to the Goldman (35) and Hodgkin and Katz (36) current relationships.

$$I_S = P_K z_S^2 \left(\frac{VF^2}{RT} \right) \left(\frac{[K]_i - [K]_o \exp(-z_S VF/RT)}{1 - \exp(-z_S VF/RT)} \right) \qquad \text{(Eq. 1)}$$

where P_K is the permeability of potassium, z, V, F, R, and T have their usual meanings, and an internal K^+ concentration of 90 mM is assumed, as reported previously (37). Permeability ratios were calculated according to the following equation.

$$\frac{P_K}{P_X} = \exp\left(-\frac{V_{rev} F}{RT}\right) \qquad \text{(Eq. 2)}$$

where P_K and P_X are the permeability of potassium and the test cation, respectively; in whole cell mode it is assumed that potassium is the only permeant ion inside the cell. Dose response curves were fit to the following function.

$$\frac{1}{1 + \left(\frac{[B]}{K_{1/2}}\right)^n} \qquad \text{(Eq. 3)}$$

where $[B]$ is the concentration of the blocker, $K_{1/2}$ is the concentration of the blocker required to achieve 50% inhibition, and n is the Hill coefficient. The voltage dependence of block was modeled by a simplification of the approach of Woodhull (38) according to the following equation.

$$\frac{I}{I_{max}} = \left[\frac{[B]}{K_{1/2}} \exp \frac{-z\delta FV}{RT} + 1 \right]^{-1} \qquad \text{(Eq. 4)}$$

where z and δ represent charge on the blocker and the apparent electrical distance traversed by the blocking particle to reach its receptor site.

RESULTS

Kcnk3 Encodes a Two P Domain Subunit with Four Predicted Transmembrane Segments—Three independent cDNA clones for *Kcnk3* isolated from a murine cardiac library were found to be identical (accession number AF065162) (24). Relative to the predicted initiator methionine, the cDNA contains an A in position −3 and a termination codon 209 bp upstream with no additional ATG triplets in the intervening sequence. The open reading frame is 1227 bp, and secondary structure analyses predict a protein of 409 amino acids with two classical P domains (2P) bounded by hydrophobic segments that suggest the presence of four transmembrane segments (4TM) (Fig. 1*A*).
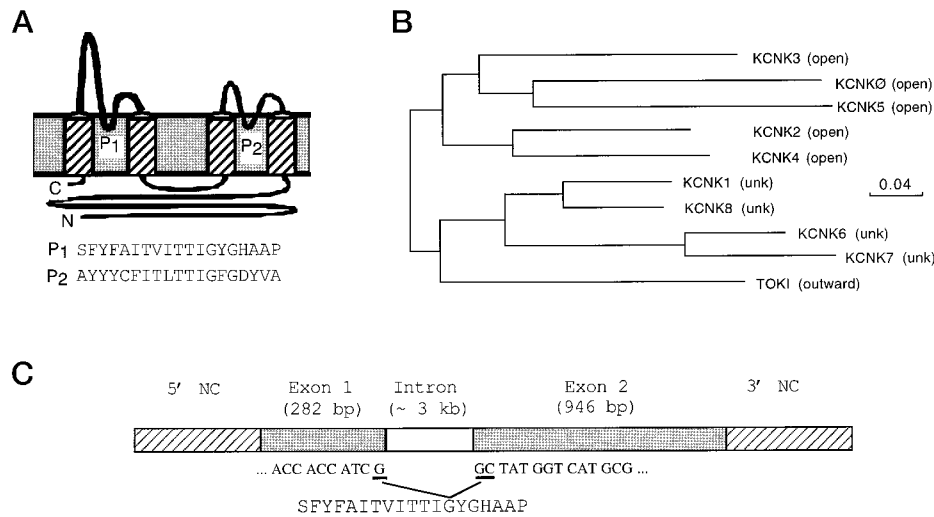
FIG. 1. **Predicted topology, gene structure, and relation to other KCNK channels.** *A*, predicted membrane topology of Kcnk3 (based on average free energy for transfer to water with a window of 20 amino acids) and amino acids in each of the two P domains. *B*, maximum likelihood tree for the relationship among the second P domains of 10 predicted two P domain potassium channel subunits. The *scale bar* indicates predicted genetic distance. Each subtype has a bootstrap value of 100/100. cDNA sequences are deposited under the following accession numbers: KCNKØ (*D. melanogaster*, ORK1, U55321), KCNK1 (human OHO/TWIK, U76996), KCNK2 (human TPKC1/TREK, AF004711), Kcnk3 (murine OAT1/TASK1/TBAK, AF065162), Kcnk4 (murine TRAAK, AF056492), KCNK5 (human, AF084830), Kcnk6 (murine, AF158234), Kcnk7 (murine, AF110522), KCNK8 (human, AF134149), and TOK1 (*Saccharomyces cerevisiae*, U28005). Alignments were performed by ClustalW 1.6 with Blossum algorithms with default gap opening and extension penalties and TOK1 as outgroup. Genes names as assigned by the Genome Data Base Nomenclature Committee and the Human Genome Organization. *C*, genomic organization of *Kcnk3* (accession numbers AF241798 and AF242508). The cDNA sequence across the exon 1/2 boundary and predicted P_1 amino acids are indicated. *NC*, noncoding.

A 2P/4TM topology is consistent with the absence of a recognizable leader sequence, the external disposition of one consensus site for *N*-linked glycosylation, and an internal location for two sites for protein kinase C, two for protein kinase A, three for calcium-calmodulin kinase II, one for tyrosine kinase, and a carboxyl-terminal PDZ consensus motif.

Alignments of the P domains for subunits predicted to have two P domains reveals that Kcnk3 is most similar to the open and outward rectifiers (KCNKØ, KCNK2, Kcnk4, and KCNK5), more distantly related to clones with as yet undefined function (KCNK1, Kcnk6, Kcnk7, and KCNK8) and most distinct from the outward rectifier of yeast cells, TOK1 (Fig. 1*B*). Homology among the genes is insignificant except for the P domain segments where pairs can achieve ~30% identity.

We verified the predicted *Kcnk3* cDNA sequence by comparison to the genomic DNA sequence (accession numbers AF241798 and AF242508). Three *Kcnk3* genomic clones were identified by polymerase chain reaction screening, and one was studied in detail by restriction enzyme analysis, Southern blotting, and limited nucleotide sequencing. The region of this clone containing the *Kcnk3* gene, including 5′and 3′-untranslated sequences and the coding region, were sequenced on both strands. Comparison of cDNA and genomic sequences showed that *Kcnk3* is a two exon gene spread over ~21 kb (Fig. 1*C*). Evaluation of the exon/intron boundaries revealed the AG:GT rule was not violated and that no AG nucleotide pairs were present in the 15 bp upstream of the 3′ (acceptor) splice junction. The single exon/intron boundary is located at a functionally critical position in the channel, in the midst of the selectivity filter "signature sequence" (G YG) of the first P domain.

Kcnk3 mRNA Is Abundant in Murine Cardiac Ventricle—Northern blot analysis using an 801-bp *Kcnk3* cDNA fragment as probe detected a strong signal in heart with less abundant message in lung and brain (Fig. 2*A*). Only a single band at ~3.8 kb was detected. Faint signals were visualized after exposure for extended periods in skeletal muscle and kidney (not shown). When the distribution of *Kcnk3* message in mouse heart was examined by *in situ* hybridization, a strong, specific signal was apparent throughout both ventricles with the antisense probe

(Fig. 2*C*). A weak antisense signal was also visualized in the atria, indicating a lower level of transcript in those cells. Because this localization was at odds with prior reports (26), we evaluated the cardiac expression pattern of Kcnk3 protein.

Kcnk3 Protein Is Prominent in Ventricle—Anti-peptide antibodies were used to visualize Kcnk3 protein in homogenates of murine atrial and ventricular tissue (Fig. 2*D*). A strong signal near the predicted mass for Kcnk3 was apparent in ventricular samples (Fig. 2*D*, *lane 1*); a weaker signal was found in atrial preparations despite the presence of similar amount of total protein in the lane (Fig. 2*D*, *lane 2*). The signal was demonstrated to be specific for Kcnk3 protein because it was competitively depleted by co-incubation with the peptide fragment recognized by the antiserum (Fig. 2*D*, *lanes 3* and *4*).

Kcnk3 Protein Forms Potassium-selective, Openly Rectifying Ion Channels—When *Kcnk3* cRNA was injected into *X. laevis* oocytes, a new current was observed by two-electrode voltage clamp (Fig. 3*A*) that was not present in control cells. In response to changes in voltage, the current rose to a new steady state level. Once activated, inactivation was not observed (10 s pulses; not shown). At physiological levels of bath potassium (5 mM) and pH (7.4), the channel passed large outward currents with depolarizing voltage steps but only small inward currents at hyperpolarized potentials (Fig. 3*A*, *left panel*). Increasing external potassium concentration produced a shift in reversal potential and large inward currents (Fig. 3, *A* and *B*). The change in reversal potential indicated that the channel was selective for potassium over sodium and chloride. Thus, increasing external potassium levels from 5 to 100 mM (by isotonic substitution of NaCl with KCl) produced a shift in reversal potential of 56 ± 3 mV/10-fold change in potassium (Fig. 3*C*) in good agreement with the Nernst relation, which predicts an ~58 mV change for a perfectly selective channel under these conditions.

Changes in current-voltage relationships with altered external potassium indicated that Kcnk3 channels were openly rectifying. Thus, inward currents were smaller than outward currents when external potassium was low and increased to equal magnitude when potassium levels were approximately the
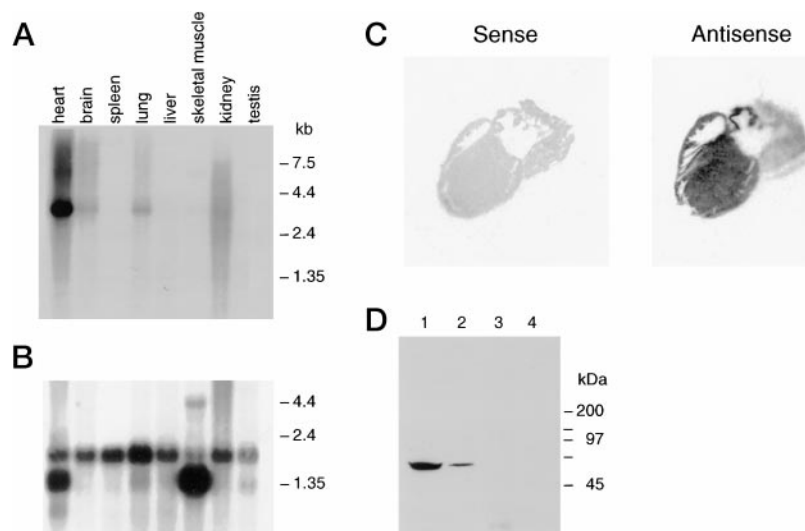
FIG. 2. **Kcnk3 message and protein are present in murine cardiac ventricular cells.** *A*, Northern blot analysis. Samples of 2 μg of poly(A)$^+$ mRNA from various murine tissues were hybridized to a [^{32}P]dCTP-labeled 801-bp murine KCKN3 cDNA fragment. Abundant message of ~3.8 kb was detected in heart, with lower amounts detected in brain and lung. *B*, the blot used in *A* was stripped and hybridized to a [^{32}P]dCTP-labeled β-actin cDNA probe as a control for loading. Note that in skeletal and cardiac muscle, both the expected 1.6–1.8- and 2.0-kb signals are seen after hybridization with this probe. *C*, *in situ* hybridization of mouse heart with a ^{35}S-UTP-labeled 801-bp murine *Kcnk3* cDNA fragment demonstrates *Kcnk3* message in murine ventricular tissue. *D*, anti-KCNK3 antibodies and Western blot analysis show that Kcnk3 protein is prominent in murine ventricular tissue. Triton X-100 extracted ventricle or atrium homogenate (100 μg) was loaded in each lane of a 10% SDS-polyacrylamide gel and probed with anti-KCNK3 antibody (APC024). *Lanes 1* and *3*, ventricular cell lysates; *lanes 2* and *4*, atrial cell lysates; *lanes 3* and *4* show loss of the specific signal upon co-incubation of control antigen peptide with KCNK3 antibody (1 μg peptide/1 μg antibody) prior to probing.

same across the membrane (Fig. 3, *A* and *B*). This behavior was reasonably well approximated by the Goldman-Hodgkin-Katz relation (Equation 1) for current through across an ion-selective partition at differing transmembrane gradients of permeant ion (Fig. 3*B*). It was notable that Equation 1 failed to approximate the experimental data at 5 mM bath potassium because outward currents were smaller than predicted. This was subsequently explained by potassium-dependent proton inhibition of Kcnk3 channel currents (see below).

Kcnk3 channels exhibit an Eisenman type III permeability series (Fig. 3*D*). To assess relative permeability compared with potassium (the predominant internal permeant ion), a test cation replaced the sodium and potassium in the bath solution to achieve a pseudo bi-ionic condition in whole cell mode and Equation 2 was used. Permeability was highest for rubidium (1.1 ± 0.1, *n* = 12) and potassium (= 1), intermediate for cesium and ammonium (0.30 ± 0.02 and 0.23 ± 0.03, *n* = 8, respectively), and lowest for sodium and lithium (less than 0.031 ± 0.003 and 0.031 ± 0.002, *n* = 8, respectively). Although rubidium had a greater relative permeability than potassium its relative conductance was over 2-fold lower (Fig. 3*D*).

Proton Inhibition of Kcnk3 Channels at Physiological pH Is Potassium-sensitive—With 5 mM potassium in the bath, Kcnk3 currents were maximal at pH 8.0, significantly blocked at pH 7.4, and completely inhibited at pH 6.0 (Fig. 4*A*). Proton block was well fit to Equation 3 with a half-maximal blocking concentration (pK_a) of 7.24 ± 0.03 and a Hill coefficient of 1.02 ± 0.06, suggesting that one proton was required to block (Fig. 4*B*). As external potassium levels rose, block by protons was diminished (Fig. 4*C*); at pH 7.0, the fraction of unblocked current at 30 mV in a potassium-free bath solution was 0.32 ± 0.02 and increased to 0.54 ± 0.02, 0.73 ± 0.02 and 0.94 ± 0.02 with 5, 20, and 100 mM bath potassium, respectively. Increasing proton levels inhibited Kcnk3 channels despite elevated potassium levels (not shown). The effect of potassium on proton inhibition explained the anomalous increase in outward current seen with elevation of external potassium (Fig. 3*A*); although increasing bath potassium decreased the outward driv-

ing force for potassium flux, it also diminished proton inhibition (Fig. 4*C*) leading to an overall increase in outward current.

External Potassium Alters the Fraction of Kcnk3 Current That Is Time-dependent—The rise and fall of Kcnk3 currents showed a phase that appeared immediate and another that was delayed. In whole cell mode, ~40% of activation was judged to be time-dependent with steps from −80 to 60 mV at physiological levels of pH (7.4) and potassium (5 mM) (Fig. 5*A*). Both raising external potassium from 5 to 100 mM (Fig. 5*B*, *left panel*) and decreasing protons from pH 7.0 to 8.0 (Fig. 5*A*, *right panel*) decreased the fraction of current that was time-dependent (I_{TD}/I). Similarly, 55% of deactivating current was judged to be time-dependent with a step from 60 to −120 mV at pH 7.4 and 5 mM potassium (Fig. 5*C*), and raising external potassium (Fig. 5*D*, *left panel*) and lowering proton level (Fig. 5*D*, *right panel*) decreased the fraction of current that was time-dependent. I_{TD}/I reflects the fraction of channels closed at rest; thus, higher potassium and lower proton in the bath increased the fraction of channels that were open before the test pulse. At physiological resting potentials and ionic conditions, roughly half the Kcnk3 channels that passed current upon depolarization were already open. The effects of external potassium were consistent with the theory that increased occupancy of the external pore by potassium (either by raising bath levels or decreasing proton block) favored the open channel state.

Voltage Alters the Fraction of Time-dependent Kcnk3 Currents—Kcnk3 currents in on-cell patches showed changes with voltage consistent with altered open probability (Fig. 6). Thus, the fraction of time-dependent current decreased with more positive holding potential (from −150 to −60 mV; Fig. 6*A*, *middle panel*) or test pulse (from 0 to 60 mV; Fig. 6*A*, *right panel*), indicating opening of channels by depolarization. Deactivation showed a similar dependence on voltage; activation at positive potentials (from 0 to 60 mV; Fig. 6*B*, *middle panel*) opened more channels, increasing the fraction of current that decayed upon subsequent hyperpolarization, and more positive deactivation potential (from -150 to -60 mV; Fig. 6*B*, *right*
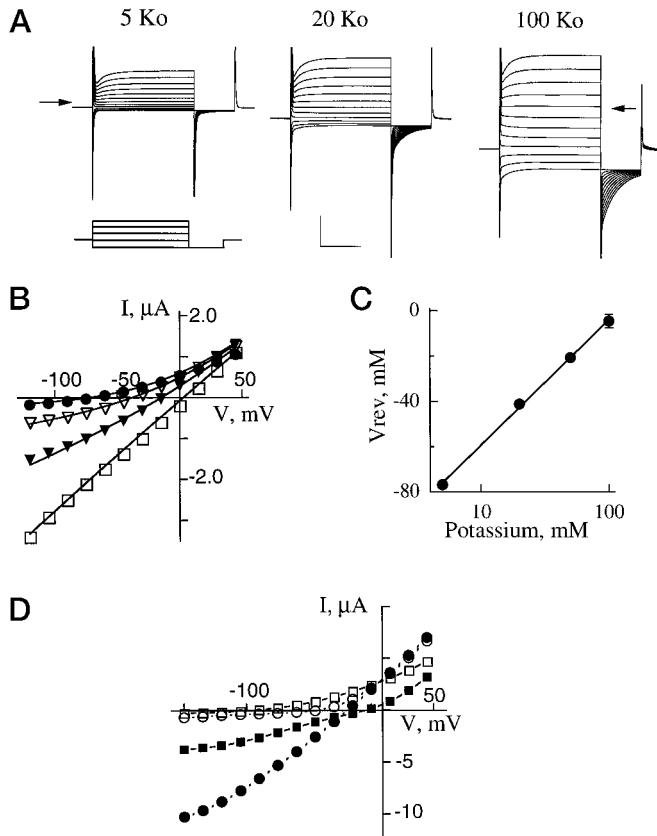
FIG. 3. **Kcnk3 channels are openly rectifying and potassium-selective.** Kcnk3 whole cell currents were assessed in oocytes by two-electrode voltage clamp with pulses from a holding voltage of −80 mV with 50 ms steps from −120 to 45 mV in 15 mV increments, followed by a 20 ms step to −120 mV. A 1-s interpulse interval was used. *A*, Kcnk3 currents at 5, 20, and 100 mM external potassium solutions at pH 7.4. *Scale bars* represent 2 μA and 20 ms. *Arrows* indicate the zero current level. *B*, steady state current-voltage relations in 5 (*closed circle*), 20 (*open triangle*), 50 (*closed triangle*), and 100 mM (*open box*) potassium solution for a single oocyte. The *solid lines* are drawn according to Equation 2. *C*, the reversal potential of Kcnk3 currents was determined with 5, 20, 50, and 100 mM potassium solutions (mean ± S.E., $n = 6$). Linear regression gave a shift of 56 ± 3 mV/10-fold change in potassium concentration. *D*, Kcnk3 steady state current-voltage relationships for groups of oocytes studied with 100 mM rubidium, potassium (*filled circle*), rubidium (*filled square*), cesium (*open circle*), or lithium (*open square*) in the external solution. The conclusion that permeability assessments were not significantly altered by native conductances was supported by the magnitude of Kcnk3 currents in cells expressing the channel and that absence of less selective pathways (*C*).

FIG. 4. **Kcnk3 channels are inhibited by protons at physiological pH.** Kcnk3 currents were studied in whole cell mode at the indicated pH and potassium solutions. Oocyte membrane potential was held at −80 mV and pulsed from −120 to +45 mV in 15 mV voltage steps for 50 ms, followed by a 20 ms step to −120 mV. A 1-s interpulse interval was used. *A*, representative oocyte expressing Kcnk3 exposed to varying pH with 5 mM potassium bath solution. *Scale bars* represent 1 μA and 20 ms. *B*, dependence of Kcnk3 currents at 0 mV on bath pH (mean ± S.E.) for groups of five cells in 5 mM potassium solution normalized to pH 8.0. The *solid line* represents a fit of the data to Equation 3. A pK_a of 7.24 ± 0.03 and a Hill coefficient of 1.02 ± 0.06 were obtained. *C*, inhibition of Kcnk3 current by protons was potassium-dependent. Steady state current-voltage relationships for pH 8.0 (*filled circle*) and pH 7.0 (*open circle*) at indicated levels of bath potassium (in mM).

panel) decreased I_{TD}/I, presumably by increasing the number of channels that stayed open.

Voltage Influences the Kinetics of Time-dependent Kcnk3 Currents—Activation and deactivation were well approximated by single exponential relationships, and both rates showed a weak dependence on voltage. The rate of activation was greater at more positive test potentials (Fig. 6B), although deactivation was faster at more negative voltages (Fig. 6D). With 5 mM external potassium at pH 7.4, the time constant (τ) for the rise in the current (with a step from −80 to 45 mV) was 4.4 ± 0.5 ms and showed an *e*-fold change per ~250 mV over this voltage range (Fig. 6B). This rate of was largely insensitive to both external potassium and pH. Thus, τ with 20 mM potassium at pH 7.4 was 4.1 ± 0.2 ms ($n = 3$), whereas it was 4.4 ± 0.4 and 4.3 ± 0.6 ms at 5 mM potassium at pH 8.0 ($n = 4$) and pH 7.0 ($n = 4$), respectively.

The time constant for current decay was 5.0 ± 0.2 ms ($n = 5$) at −120 mV and changed *e*-fold per ~500 mV over this range of potentials (Fig. 6D). Another measure of deactivation rate was
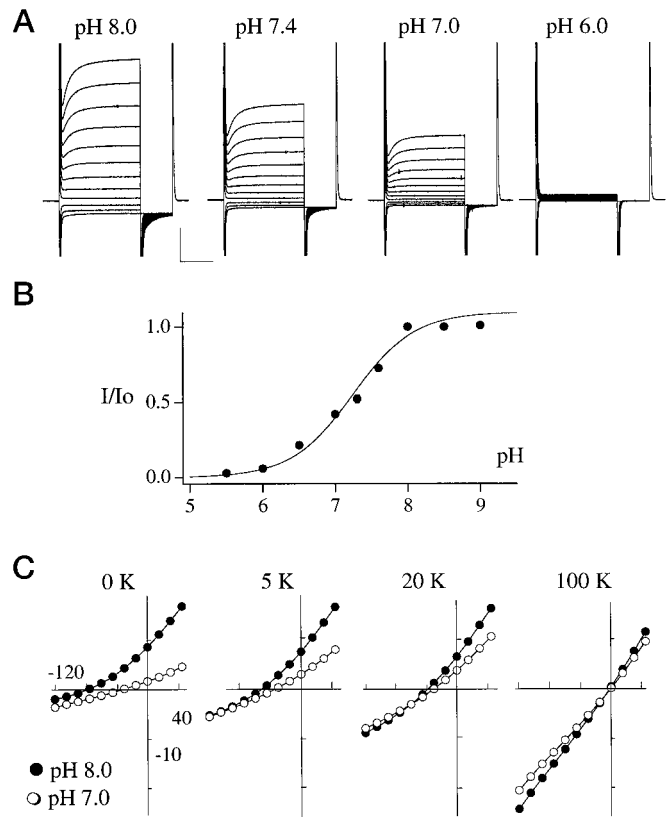
the time required at −80 mV to recover an initial ratio of immediate to time-dependent current as measured by activation (Fig. 6E). The recovery time constant at −80 mV was 5.7 ± 0.3 ms ($n = 3$), similar to the deactivation rate estimated directly at −80 mV, 5.5 ± 0.3 ms ($n = 3$).

A rough upper limit for the time course of "immediate" current development with voltage steps was determined in patch mode from the inflection point between the fall of the capacitance transient and the rise of the time-dependent current (as the immediate phase was judged to be complete by this time). By this strategy, the rise of the immediate current (with a step from −80 to 45 mV) was less than 0.25 ms (Fig. 6A), consistent with the idea that these channels were open before test pulse.

Single Kcnk3 Channels and Unitary Conductance—A new potassium channel was observed at the single channel level in oocytes expressing *Kcnk3*. Open infrequently, its slope conductance was estimated to be 11 ± 1 pS in on-cell patches with approximately symmetric 100 mM potassium (Fig. 7, *A* and *B*, *left panel*). Although ~70% of openings were to this level, ~30% were to a conductance level ~1.6-fold larger (based on 11,000 single channel transitions). This suggested our estimate of unitary conductance was for a dominant substate (Fig. 7B, *middle panel*). Unitary conductance estimated by noise variance analysis was 10 ± 1 pS (Figs. 7C).
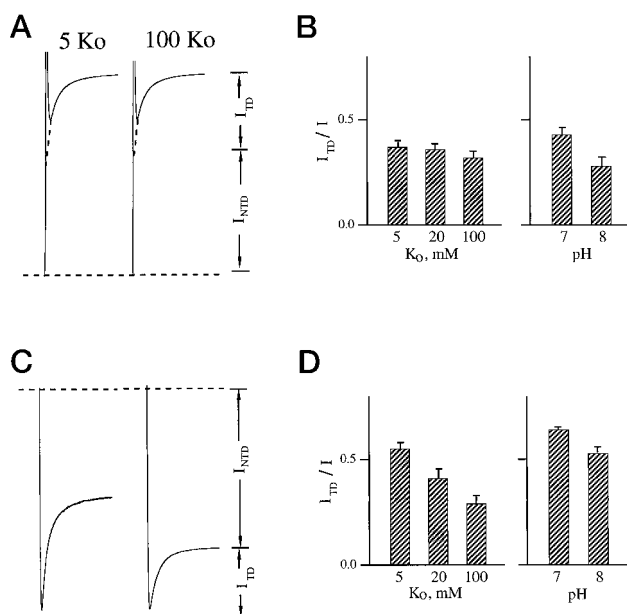
FIG. 5. **The fraction of time-dependent Kcnk3 current is potassium and pH-dependent.** *A*, activation. Kcnk3 current traces measured in whole cell mode in 5 and 100 mM potassium solution, pH 7.4. Oocyte membrane potential was held at −80 mV and pulsed to 60 mV for 50 ms. Currents are normalized to peak (8–10 μA). I_{TD} and I_{NTD} represent the time-dependent and non-time-dependent components of the current. Steady state and initial currents (see *dashed line*) were estimated using a single exponential fit of the data. *B*, activation. The fraction of time-dependent current assessed as in *A* with 5, 20, and 100 mM potassium and pH 7.4 or 5 mM potassium and pH 7.0 or 8.0. Mean ± S.E. for 3–6 cells. *C*, deactivation. Kcnk3 current traces in whole cell mode in 5 and 100 mM potassium solution, pH 7.4. Oocyte membrane potential was held at 60 mV and pulsed to −120 mV for 50 ms. Currents are normalized to peak (−2 to −13 μA). I_{TD} and I_{NTD} and fits are as in *A*. *D*, deactivation. The fraction of time-dependent current assessed as in *C* with 5, 20, and 100 mM potassium and pH 7.4 or 5 mM potassium and pH 7.0 or 8.0. Mean ± S.E. for 3–6 cells.

Single Kcnk3 channels studied in outside-out patch mode recapitulated observations made macroscopically; single channels were selective for potassium, openly rectifying, and sensitive to external pH (Fig. 8*A*). Thus, Kcnk3 channels were observed at both depolarized and hyperpolarized voltages in approximately symmetric 100 mM potassium with a reversal potential of ~0 mV (Fig. 8*A*, *left panel*). When external potassium was lowered to 5 mM, no inward currents were observed, and the reversal potential was ~−80 mV, close to the equilibrium reversal potential for potassium (Fig. 8*A*, *middle panel*). Lowering pH from 7.4 to 6.0 at 5 mM potassium completely inhibited single-channel activity (Fig. 8*A*, *right panel*) in a reversible manner (not shown).

Latency to First Opening and Open Probability of Single Kcnk3 Channels—The response of single channels to voltage was assessed by holding outside-out patches at the reversal potential for potassium (−40 mV in this case) and repeatedly stepping to +40 and then −120 mV, test voltages with equal but opposite driving force for potassium. Most traces were null with no openings or closings observed (Fig. 8*B*, *trace 5*); others showed evidence for brief openings with depolarization (Fig. 8*B*, *traces 1* and *3*) or hyperpolarization (Fig. 8*B*, *traces 2* and *4*). The ratio of openings to the two conductance levels was similar to that observed in steady state recordings (~7:3, not shown).

In on-cell patches at −120 mV with approximately symmetric 100 mM potassium (Fig. 7*A*) open probability was ~0.04 ± 0.01 at steady state. Dwell time for openings were well approximated by a single time constant of 0.3 ± 0.1 ms, suggesting that open times for the two conductance levels were similar

(Fig. 7*B*, *right panel*). Closed time distributions were best fit by two time constants representing closed states with mean dwell times of ~5 and 65 ms, with relative frequencies of 19 and 81%, respectively (Fig. 7*B*, *right panel*).

Important sources of error in these estimates were uncertainty about whether more than one channel was present in a patch (in which case open probability estimates were too large) and missed brief openings as the minimal detectable event was 90 μs at the filter frequency employed (2 kHz) and mean open time was ~300 μs (tending to depress estimates of open probability). Errors because of unappreciated channels with open probability ~1 were ruled out because lowering pH had no effect on current base line. Finally, one of seven patches thought to have a single Kcnk3 channel showed an P_o of ~0.14; this patch was excluded from analyses but may have represented Kcnk3 channels in a different functional mode.

Modulation of Kcnk3 Currents—The presence of multiple regulatory consensus sites in the carboxyl-terminal segment of Kcnk3 and its low open probability suggested that the channel might be down-regulated in oocytes. Moreover, whole cell Kcnk3 currents tended to slowly "run down," ~15% over 30 min (Table I). Therefore, a variety of common potassium channel inhibitors and activators were evaluated in the presence of 20 mM external potassium to permit ready measurement of both inward and outward currents (Table I). Only depolarizing voltage steps were found to increase open probability significantly. Kcnk3 channels were found to be relatively insensitive to common blockers added to the bath (tetraethylammonium, 4-aminopyridine, and glibencamide and sensitive to amiodorone and barium). PMA (50 nM), an activator of protein kinase C, had no rapid effect (10 min) but decreased current by ~⅓ over 30 min (Table I). Bisindolylmaleimide I (5 μM), an inhibitor of protein kinase C, slowly increased currents ~⅓ over 30 min and suppressed PMA-induced down-regulation when the agents were applied together (Table I). Activation of protein kinase A by 20 μM forskolin and 1 mM IBMX decreased current by ~40%, although PKA inhibitor H-89 at a standard dose (5 μM) had no effect (Table I). Small to moderate decreases in Kcnk3 currents were also observed with manipulations known to activate K_{ATP} channels (3 mM sodium azide) (39), Kcnk4 channels (100 μM arachadonic acid) (17), and a native leak channel (decreased oxygen tension achieved by purging the bath solution with nitrogen) (7) (Table I). Minimal changes in current were observed when bath osmotic and ionic strength were increased, bath calcium and/or magnesium were increased or removed, calcium was eliminated and 5 mM EGTA added, ultra-pure potassium was employed as a sole source of external monovalent cations, or the volatile anesthetics halothane or chloroform were applied at supra-therapeutic levels (Table I). These manipulations did not significantly alter the fraction of time-dependent current at 60 or −120 mV (not shown).

DISCUSSION

The superfamily of genes encoding potassium channel subunits with two P domains has emerged with remarkable speed since the cloning of TOK1 (with a predicted 2P/8TM topology) (40) and KCNKØ (with a predicted 2P/4TM topology) (13). At present, more than 70 genes are listed in public data bases. Mammalian genes, now identified as *KCNK1–9* by the Human Genome Organization, all have a predicted 2P/4TM topology. Thus far, KCNK channels that function are "leak" conductances; they have a non-zero open probability across the physiological voltage range. KCNK2 and KCNK5 are outward rectifiers, a phenotype first observed for TOK1 (40–42); under symmetric ionic conditions these pass large outward potassium currents and small inward potassium currents (16, 18, 43). KCNKØ, Kcnk3, and Kcnk4 are open rectifiers, showing linear
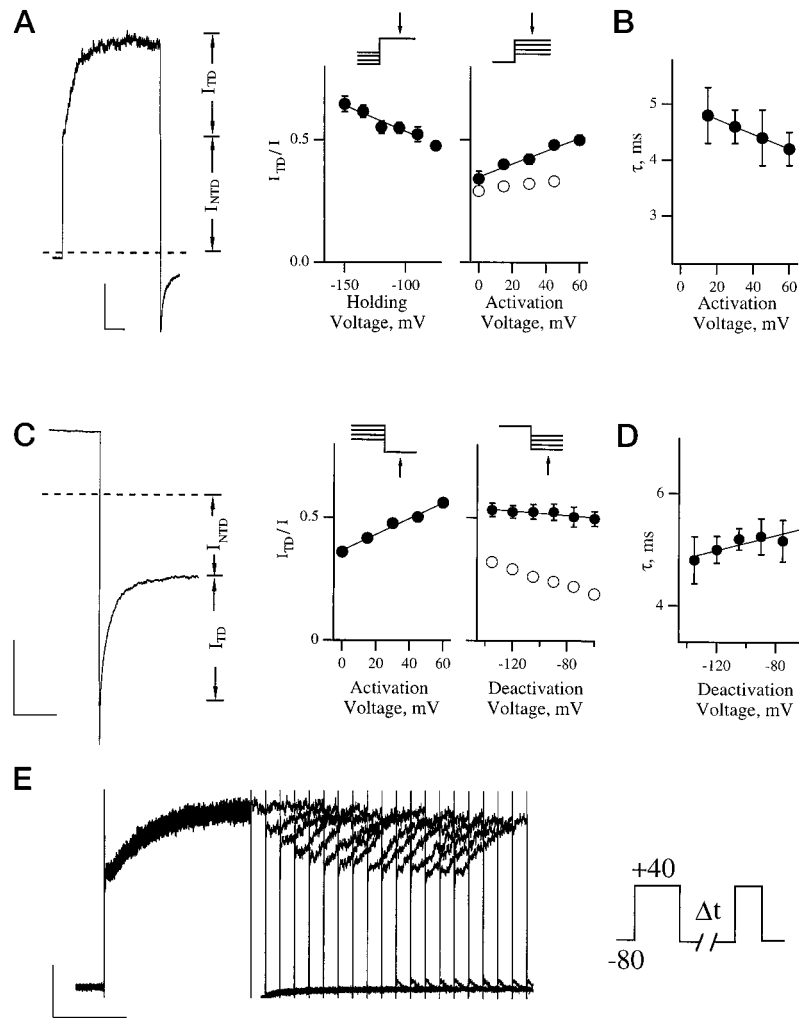
FIG. 6. **Activation and deactivation of Kcnk3 channels are weakly voltage-dependent.** *A*, activation. *Left panel*, Kcnk3 current traces in on-cell patches pulsed for 50 ms from −80 mV to 60 mV (followed by a step to −120 mV) with 5 mM potassium, pH 7.4 in the pipette. I_{TD} and I_{NTD} represent the time-dependent and non-time-dependent components of the current. The *dotted line* indicates zero current. *Scale bars* represent 100 pA and 10 ms. *Middle panel*, holding voltage alters the fraction of time-dependent Kcnk3 current measured at 40 mV for groups of 5 cells (mean ± S.E.). Steady state and initial currents were estimated using a single exponential fit of the data. *Right panel*, activation voltage alters the fraction of time-dependent Kcnk3 current for groups of 5 cells (mean ± S.E.). The *open symbols* are the ratios by the same protocol in whole cell mode. *B*, the command voltage alters the time course of activation. The time constant (τ) for activation at various voltages for groups of five cells studied as in *A* and fit with a single exponential of the form a + b*exp (−x/τ). *C*, deactivation. *Left panel*, Kcnk3 current traces in on-cell patches pulsed for 50 ms from a holding potential of 60 mV to −120 mV with 100 mM potassium, pH 7.4, in the pipette. Otherwise conditions are as in *A*. *Scale bars* represent 100 pA and 20 ms. *Middle panel*, prior activation voltage alters the fraction of time-dependent Kcnk3 current at −120 mV for groups of 5 cells (mean ± S.E.). Steady state and initial currents were estimated using a single exponential fit of the data. *Right panel*, deactivation voltage alters the fraction of time-dependent Kcnk3 current for groups of 5 cells (mean ± S.E.). The *open symbols* are the ratios by the same protocol in whole cell mode. *D*, the command voltage alters the time course of deactivation. Time constant (τ) for deactivation at various voltages for groups of five cells were studied as in the *right panel* in *C* and fit with a single exponential as in *B*. *E*, deactivation. The time course of recovery from prior activation was evaluated in on-cell mode by increasing the time between two successive 50 ms activating test pulses to 40 mV from −80 mV with 5 mM potassium, pH 7.4, solution in the pipette; the two pulses were separated by intervals of 2–100 ms, and traces are superimposed. *Scale bars* represent 100 pA and 20 ms.

current-voltage relationships under symmetric conditions and Goldman rectification (35, 36) when potassium levels are unequal across the membrane (13, 17, 24, 26, 27, 44).[2] Kcnk9 is an inwardly rectifying clone (23), whereas KCNK1, Kcnk6, Kcnk7, and KCNK8 do not show reproducible function (16, 19–22). Previously accessible only in native cells, cloned leak channels are now available for detailed evaluation under controlled conditions.

Genomic Organization—Kcnk3 has an intron in the first P domain. This boundary is located at the same location in KC-NKØ, *KCNK2*, *Kcnk4*, and *Kcnk5* based on their genomic sequences as reported in the GenBank[TM] data base of NCBI[4] and

Kcnk7[5] as well as 20 predicted two P domain channel genes in the nematode *Caenorhabditis elegans* (45). Maintenance of this organization suggests either that this noncoding region serves an important regulatory role or that its natural deletion is infrequently propagated because random excision risks damage to the signature sequence residues that are required for function. That the genomic organization of *Kcnk7*,[5] which is nonfunctional in experimental cells, is like that of *Kcnk3* indicates the intron/exon boundary does not designate which KCNK isolates will show function.

The functional attributes we determine for Kcnk3 differ in a

[4] N. Zilberberg and S. A. N. Goldstein, unpublished observation.

[5] D. Bockenhauer, M. A. Nimmakayalu, D. C. Ward, S. A. N. Goldstein, and P. G. Gallagher, submitted for publication.
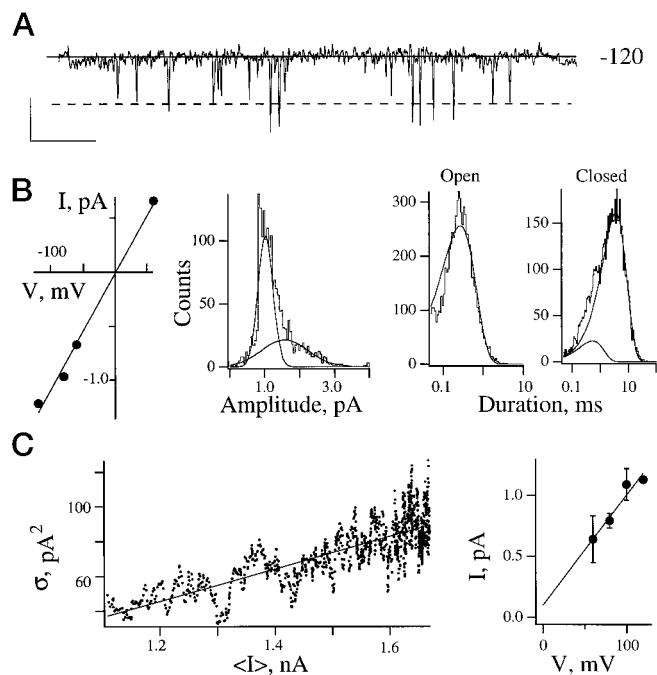
Fig. 7. **Single Kcnk3 channel conductance.** Single channel currents were recorded in an on-cell patches with 100 mM potassium solution in the pipette. *A*, representative single Kcnk3 channel at −120 mV. The *solid line* indicates zero current, and the *dotted line* indicates major open channel level. The *scale bar* represents 1 pA and 50 ms. Data were filtered at 2 kHz and sampled at 10 kHz. *B*, *left panel*, the unitary current-voltage relationship estimates a conductance of 11 ± 1 pS. *Middle panel*, single channel data analyzed off-line allowed construction of histograms using a 50% crossing method (21); ∼70% of openings were to a mean value of 1.2 pA, the other was to 1.6 pA, corresponding to 10 and 13 pS. *Right panel*, representative open and closed time histogram for single Kcnk3 channels at −120 mV in 100 mM potassium solution; the histograms represent 20 s of data from six single channel patches (20,000 events) evaluated as in *A* with maximum-likelihood fits to the data. *C*, *left panel*, single channel conductance was estimated by noise variance analysis in four patches pulsed 300 times to 80 mV for 15 ms from a holding voltage of −80 mV. Current variance and mean were calculated. For a channel with low open probability the slope of the current variance-mean relationship gives a valid approximation of unitary current. *Right panel*, current-voltage relationship for variance analyzed at different voltages offered an estimate of single channel conductance of 10 ± 1 pS.

number of respects from those reported by others; most notable, they did not observe time-dependent currents (26, 27, 44). Sequence differences, although minor, may explain functional discrepancies between the clones under study. Based on combined cDNA and genomic sequencing, it appears that the *Kcnk3* variant we study is derived from the same gene as TASK1 (26) and TBAK1 (27). Alternative splicing cannot explain variations among the three cDNA sequences. Thus, these differences must result from RNA editing (46), or they are due to sequence errors introduced during reverse transcription or polymerase chain reaction.

Kcnk3 Channel Protein: a Potential Correlate of Cardiac I_{Kp}—Whereas we visualize *Kcnk3* transcripts throughout the heart with a predominance in ventricle by *in situ* hybridization (Fig. 2*B*), others find message only in cardiac atria (26). Here we support ventricular localization by direct demonstration that Kcnk3 protein is also in ventricular tissue and at lower levels in atrial samples (Fig. 2*C*). The conclusion that Kcnk3 channels function in cardiac myocytes (rather than nonmuscular cells) is supported by a report that *Kcnk3* message can be amplified from single cardiac myocytes by polymerase chain reaction (27), rare observation of single channels in rat ventricular myocytes with the same unitary conductance as murine Kcnk3 (47), and suppression of mouse ventricular currents by
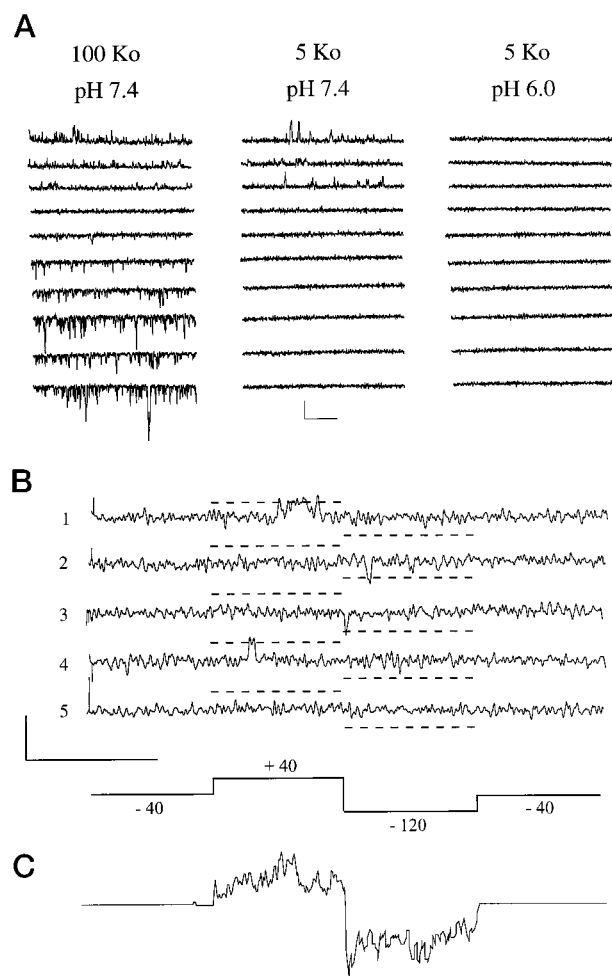

Fig. 8. **Single Kcnk3 channel first latency and open probability.** Single Kcnk3 channels were studied in outside-out patches with 100 mM potassium in the pipette. *A*, a patch with multiple Kcnk3 channels at various bath conditions. *Left panel*, 100 mM potassium at pH 7.4. *Middle panel*, 5 mM potassium at pH 7.4. *Right panel*, 5 mM potassium at pH 6.0. *Scale bars* represent 2 pA and 100 ms. *B*, representative single channel patch; traces elicited by depolarization from −40 to 40 mV for 50 ms, followed by a 50-ms step to −120 mV prior to returning to the holding potential with 20 mM potassium, pH 7.4, in the bath. The driving force was similar for inward and outward potassium currents at these test potentials. *Scale bars* represent 1 pA and 50 ms. *C*, an ensemble average of 300 pulses as in *B*. In 75% of traces no openings or closings were observed (as in *B*, *trace 5*).

Kcnk3 antisense oligonucleotides.[6]

Currents in native cells with attributes similar to those we delineate for Kcnk3 channels have been reported (8–12, 28). Like Kcnk3, I_{Kp} in guinea pig cardiac myocytes is prominent in ventricle, activates rapidly, and does not inactivate with sustained depolarization (8, 9). Moreover, I_{Kp} is insensitive to external tetraethylammonium and 4-aminopyridine and sensitive to external barium (8); the effect of low pH on guinea pig I_{Kp} has not been reported. Although differences between I_{Kp} and Kcnk3 in open probability and barium block argue against identity, species differences in homologous potassium channels is well recognized (48).

Leak channels remain active at all potentials in contrast to inwardly rectifying cardiac potassium channels (49, 50). Thus, Kcnk3 channels are expected to contribute not only to establishing resting membrane potential but to the height and length of action potentials and, therefore, the duration of myo-

---

[6] C. M. B. Lopes, M. Apkon, and S. A. N. Goldstein, unpublished observation.

TABLE I
Effects of various agents on Kenk3 current magnitude

Whole cell current was measured before and at steady state after exposure to the indicated agent except for PMA, which was studied at 30 min by pulsing from −80 to 30 mV for 50 ms with interpulse interval of 2 or 30 s (PMA, bisindolylmaleimide, forskolin, H-89, azide, and hypoxia); all effects were reversible except for those of arachidonic acid. zδ was calculated by Equation. The efficacy of the H-89 solution was confirmed by its effects on KCNKØ channels (not shown).

Treatment (dose, cells studied)	Percent change $\pm$ S.E.
None ($n = 6$)	-4 ± 2 (10 min); -14 ± 4 (30 min)
TEA (75 mM, $n = 8$)	-23 ± 2 (zδ $= 0.00 \pm 0.01$)
4-AP (2 mM, $n = 7$)	-36 ± 4 (zδ $= 0.00 \pm 0.09$)
Glibencamide (10 μM, $n = 4$)[a]	$+3 \pm 1$
Amiodorone (10 μM, $n = 5$)[a]	-43 ± 4 (zδ $= 0.12 \pm 0.03$)
Barium (0.5 mM, $n = 3$)	-64 ± 5 (-120 mV) (zδ $= 0.45 \pm 0.01$)
Proton (pH 7.3/5 mM KCl, $n = 15$)[a]	-52 ± 2 (0 mV)
Calcium-free ($n = 5$)	-16 ± 6
Calcium added (2 mM, $n = 4$)	$+8 \pm 3$
Magnesium-free ($n = 4$)	-10 ± 4
Magnesium added (2 mM, $n = 4$)	$+1 \pm 5$
Calcium-free + EGTA (5 mM, $n = 4$)	$+7 \pm 1$
Calcium and magnesium-free ($n = 4$)	-12 ± 9
Ultra-pure potassium (100 mM, $n = 3$)	$+4 \pm 1$
PMA (50 nM, $n = 9$)	-13 ± 4 (10 min); -46 ± 5 (30 min)
Bisindolylmaleimide I (5 μM, $n = 5$)	$+28 \pm 3$ (30 min)
Bisindolylmaleimide I + PMA ($n = 4$)	$+9 \pm 2$ (30 min)
Forskolin (20 μM) + IBMX (1 mM, $n = 3$)	-43 ± 6
H-89 (5 μM, $n = 4$)	-5 ± 2
H-89 + forskolin + IBMX ($n = 3$)	-46 ± 5
Arachidonic acid (100 μM, $n = 4$)	-74 ± 3
Sodium azide (3 mM, $n = 6$)	-18 ± 3
Hypoxia (O$_2$ ~5 torr, $n = 5$)	-19 ± 3
Hyperosmotic (100 mM added NaCl, $n = 4$)	$+6 \pm 7$
Halothane (0.35 mM, 3 MAC, $n = 3$)	$+17 \pm 2$
Chloroform (1.3 mM, 2 MAC, $n = 3$)	-15 ± 2

[a] These agents were evaluated in 5 mM external potassium; all others were evaluated in 20 mM potassium solution ("Materials and Methods").

cardial contraction. Indeed, the function of pH-sensitive leak potassium conductance has been recognized in native cardiac cells (51–53).

Kcnk3 Shows Potassium-dependent Proton Block—A key property of Kcnk3 channels is their sensitivity to changes in external pH in the physiological range. Here we show that proton block is more effective at lower external potassium (Fig. 4). This served to explain the anomalous increase in outward current observed as external potassium level is elevated. The mechanism of potassium-dependent, proton block is the subject of another report.[7]

Time-dependent Changes in Kcnk3 Open Probability with Voltage Steps—Classical voltage-gated potassium channels sense changes in membrane potential via a transmembrane segment that has multiple basic residues (54–57). Shaker channels show a half-maximal activation voltage of ~0 mV and an *e*-fold change in open probability per ~25 mV (these parameters are insensitive to potassium reversal potential or absolute level). Voltage-dependent changes in Shaker current magnitude take time because they result from changes in channel conformation. Immediate increases in current (seen when channels open before a voltage step) are rarely observed with voltage-gated channels in native cells for two reasons: resting membrane potential is usually below the voltage required for opening and voltage steps that open channels also favor their entry into a nonconducting conformation, the inactivate state.

Kcnk3 manifests both immediate ($\tau < 0.25$ ms) and time-dependent ($\tau = $ ~5 ms) changes in current magnitude. Observation of immediate currents supports the conclusion that Kcnk3 channels open at all voltages. The fraction of open channels is sensitive to external potassium and voltage (Figs. 5 and 6) and does not appear to result from release from block. Thus, current magnitudes were not significantly altered by either elevation

or removal of bath calcium and/or magnesium, addition of EGTA, or formulation of solutions with 100 mM ultra-pure salts (Table I).

Kcnk3 channels appear to reside in at least four states (at all voltages) and to undergo a reversible voltage-dependent gating process. A simple model must include two open states of different conductance (O$_1$ and O$_2$) and two closed states that feed into the open states with time constants of 5 and 65 ms (C$_1$ and C$_2$). Single-channel recordings do not reveal whether channels traverse O$_1$ to enter O$_2$. That Kcnk3 enters a closed conformation is suggested by observation of a latency to first opening for single channels (Fig. 8), time-dependent development of current (Fig. 3), and the absence of evidence for blockade as a cause for entry into the nonconducting mode (Table I). The closed to open transition is seen to be voltage-sensitive by the effect of potential on the fraction and kinetics of time-dependent current (Figs. 5 and 6); a single rate-limiting voltage-gated step is suggested by good approximation of current relaxation with a single exponential.

Although KCNKØ was used to isolate Kcnk3 and is also a 2P/4TM open rectifier, it shows only instantaneous changes in current magnitude with voltage steps at both the single-channel and macroscopic level.[2] Conversely, TOK1 (the 2P/8TM outward rectifier) shows weak voltage dependence and sensitivity to potassium (40, 42, 58). Recently, Loukin and Saimi (59) showed that TOK1, like Kcnk3, visits two kinetically distinct closed states, a nearly open state (whose dwell time depends on membrane potential and potassium reversal potential), and a deeply closed state (responsive on voltage and external potassium). They observed that temperature had a significant effect on activation from the deep closed state but little effect on nearly open state. They concluded that the deep closed state reflected function of a channel gate, whereas the nearly open state was an effect of ions in the pore (59). A role for permeant ion occupancy of the pore in voltage-dependent gating is well recognized in chloride (60) and potassium chan-

[7] C. M. B. Lopes, F. Sesti, N. Zilberberg, M. E. Buck, and S. A. N. Goldstein, unpublished observation.

nels (54, 61, 62). Our results also suggest a role for occupancy of the pore by permeant ion in gating.

Kcnk3 Channels in Oocytes Have a Low Open Probability— Kcnk3 channels had a low open probability despite numerous experimental manipulations known to alter the opening and closing of other potassium channels (Table I). The paucity of openings does not result from block by protons because channels show low Po above pH 8.0 where they are not inhibited (Fig. 5*B*); nor is there evidence found for block by magnesium, calcium, or heavy metal contaminants (Table I). Although activation of PMA increases the open probability of KCNKØ dramatically and staurosporine closes that channel (63), these agents were only mildly inhibitory on Kcnk3. Arachidonic acid, reported to activate Kcnk4 (17, 64), also inhibited Kcnk3 (Table I). The volatile anesthetic halothane was reported to activate Kcnk3 by ~50% at doses lethal to humans (1 mM, ~5 MAC, where 1 MAC is the minimum alveolar concentration required to anesthetize half of the human population) (14, 15), and our results support the agents weak effect. The striking regulation of KCNKØ (63)[3] and the failure of KCNK1, Kcnk6, Kcnk7, and KCNK8 to show function in experimental cells suggests that an as yet unidentified regulator or channel subunit may act to increase the open probability of Kcnk3 channels.

REFERENCES

1. Jones, S. W. (1989) *Neuron* **3,** 153–161
2. Koyano, K., Tanaka, K., and Kuba, K. (1992) *J. Physiol.* **454,** 231–246
3. Schmidt, H., and Stampfli, R. (1966) *Pfluegers Arch Gesamte Physiol. Menschen Tiere* **287,** 311–325
4. Hille, B. (1973) *J. Gen. Physiol.* **61,** 669–686
5. Koh, D. S., Jonas, P., Brau, M. E., and Vogel, W. (1992) *J. Membr. Biol.* **130,** 149–162
6. Wu, J. V., Rubinstein, C. T., and Shrager, P. (1993) *J. Neurosci.* **13,** 5153–5163
7. Buckler, K. J. (1997) *J. Physiol.* **498,** 649–662
8. Backx, P. H., and Marban, E. (1993) *Circ. Res.* **72,** 890–900
9. Yue, D. T., and Marban, E. (1988) *Pfluegers Arch. Eur. J. Physiol.* **413,** 127–133
10. Van Wagoner, D. R., Pond, A. L., McCarthy, P. M., Trimmer, J. S., and Nerbonne, J. M. (1997) *Circ. Res.* **80,** 772–781
11. Boyle, W. A., and Nerbonne, J. M. (1992) *J. Gen. Physiol.* **100,** 1041–1067
12. Wang, Z., Fermini, B., and Nattel, S. (1993) *Circ. Res.* **73,** 1061–1076
13. Goldstein, S. A. N., Price, L. A., Rosenthal, D. N., and Pausch, M. H. (1996) *Proc. Natl. Acad. Sci. U. S. A.* **93,** 13256–13261
14. Patel, A. J., Honore, E., Lesage, F., Fink, M., Romey, G., and Lazdunski, M. (1999) *Nat. Neurosci.* **2,** 422–426
15. Patel, A. J., Honore, E., Maingret, F., Lesage, F., Fink, M., Duprat, F., and Lazdunski, M. (1998) *EMBO J.* **17,** 4283–4290
16. Goldstein, S. A. N., Wang, K. W., Ilan, N., and Pausch, M. (1998) *J. Mol. Med.* **76,** 13–20
17. Fink, M., Lesage, F., Duprat, F., Heurteaux, C., Reyes, R., Fosset, M., and Lazdunski, M. (1998) *EMBO J.* **17,** 3297–3308
18. Reyes, R., Duprat, F., Lesage, F., Fink, M., Salinas, M., Farman, N., and Lazdunski, M. (1998) *J. Biol. Chem.* **273,** 30863–30869
19. Pountney, D. J., Gulkarov, I., de Miera, E. V., Holmes, D., Saganich, M., Rudy, B., Artman, M., and Coetzee, W. A. (1999) *FEBS Lett.* **450,** 191–196
20. Salinas, M., Reyes, R., Lesage, F., Fosset, M., Heurteaux, C., Romey, G., and Lazdunski, M. (1999) *J. Biol. Chem.* **274,** 11751–11760
21. Colquhoun, D., and Sigworth, F. J. (1995) in *Single-channel Recording* (Sakmann, B., and Neher, E., eds) 2nd Ed., pp. 483–588, Plenum Press, New York
22. Chavez, R. A., Gray, A. T., Zhao, B. B., Kindler, C. H., Mazurek, M. J., Mehta, Y., Forsayeth, J. R., and Yost, C. S. (1999) *J. Biol. Chem.* **274,** 7887–7892
23. Kim, Y., Bang, H., and Kim, D. (2000) *Biophys. J.* **78,** 207 (abstr.)
24. Lopes, C. M. B., Gallagher, P. G., Wong, C., Buck, M., and Goldstein, S. A. N. (1998) *J. Biophys.* **74,** 44 (abstr.)
25. Manjunath, N. A., Bray-Ward, P., Goldstein, S. A. N., and Gallagher, P. G. (1999) *Cytogen. Cell Gen.* **86,** 242–243
26. Duprat, F., Lesage, F., Fink, M., Reyes, R., Heurteaux, C., and Lazdunski, M. (1997) *EMBO J.* **16,** 5464–5471
27. Kim, D., Fujita, A., Horio, Y., and Kurachi, Y. (1998) *Circ. Res.* **82,** 513–518
28. Apkon, M., and Nerbonne, J. M. (1988) *Biophys. J.* **53,** 458 (abstr.)
29. Altschul, S. F., Gish, W., Miller, W., Myers, E. W., and Lipman, D. J. (1990) *J. Mol. Biol.* **215,** 403–410
30. Chomczynski, P., and Sacchi, N. (1987) *Anal. Biochem.* **162,** 156–159
31. Pierce, J. C., Sternberg, N., and Sauer, B. (1992) *Mamm. Genome* **3,** 550–558
32. Ng, S. Y., Gunning, P., Eddy, R., Ponte, P., Leavitt, J., Shows, T., and Kedes, L. (1985) *Mol. Cell. Biol.* **5,** 2720–2732
33. Reppert, S. M., Weaver, D. R., Stehle, J. H., and Rivkees, S. A. (1991) *Mol. Endocrinol.* **5,** 1037–1048
34. Kandror, K. V., Coderre, L., Pushkin, A. V., and Pilch, P. (1995) *Biochem. J.* **307,** 383–390
35. Goldman, D. E. (1943) *J. Gen. Physiol.* **27,** 37–60
36. Hodgkin, A. L., and Katz, B. (1949) *J. Physiol.* **108,** 37–77
37. Wang, K.-W., Tai, K.-K., and Goldstein, S. A. N. (1996) *Neuron* **16,** 571–577
38. Woodhull, A. M. (1973) *J. Gen. Physiol.* **61,** 687–708
39. Tucker, S. J., Gribble, F. M., Zhao, C., Trapp, S., and Ashcroft, F. M. (1997) *Nature* **387,** 179–183
40. Ketchum, K. A., Joiner, W. J., Sellers, A. J., Kaczmarek, L. K., and Goldstein, S. A. N. (1995) *Nature* **376,** 690–695
41. Ahmed, A., Sesti, F., Ilan, N., Shih, T. M., Sturley, S. L., and Goldstein, S. A. N. (1999) *Cell* **99,** 283–291
42. Vergani, P., Miosga, T., Jarvis, S. M., and Blatt, M. R. (1997) *FEBS Lett.* **405,** 337–344
43. Fink, M., Duprat, F., Lesage, F., Reyes, R., Romey, G., Heurteaux, C., and Lazdunski, M. (1996) *EMBO J.* **15,** 6854–6862
44. Leonoudakis, D., Gray, A. T., Winegar, B. D., Kindler, C. H., Harada, M., Taylor, D. M., Chavez, R. A., Forsayeth, J. R., and Yost, C. S. (1998) *J. Neurosci.* **18,** 868–877
45. Wang, Z. W., Kunkel, M. T., Wei, A., Butler, A., and Salkoff, L. (1999) *Ann. N. Y. Acad. Sci.* **868,** 286–303
46. Egebjerg, J., Kukekov, V., and Heinemann, S. F. (1994) *Proc. Natl. Acad. Sci. U. S. A.* **91,** 10270–10274
47. Kim, Y., Bang, H., and Kim, D. (1999) *Am. J. Physiol.* **277,** H1669–H1678
48. Deal, K. K., England, S. K., and Tamkun, M. M. (1996) *Physiol. Rev.* **76,** 49–67
49. Kurachi, Y. (1985) *J. Physiol.* **366,** 365–385
50. Cleemann, L., and Morad, M. (1979) *J. Physiol.* **286,** 113–143
51. Nattel, S., Elharrar, V., Zipes, D. P., and Bailey, J. C. (1981) *Circ. Res.* **48,** 55–61
52. Kagiyama, Y., Hill, J. L., and Gettes, L. S. (1982) *Circ. Res.* **51,** 614–623
53. Boachie-Ansah, G., Kane, K. A., and Rankin, A. C. (1992) *J. Cardiovasc. Pharmacol.* **20,** 538–546
54. Yellen, G. (1998) *Quart. Rev. Biophys.* **31,** 239–295
55. Sigworth, F. J. (1994) *Quart. Rev. Biophys.* **27,** 1–40
56. Manuzzu, L. M., Moronne, M. M., and Isacoff, E. Y. (1996) *Science* **271,** 213–216
57. Yang, N., and Horn, R. (1995) *Neuron* **15,** 213–218
58. Vergani, P., Hamilton, D., Jarvis, S., and Blatt, M. R. (1998) *EMBO J.* **17,** 7190–7198
59. Loukin, S. H., and Saimi, Y. (1999) *Biophys. J.* **77,** 3060–3070
60. Chen, T. Y., and Miller, C. (1996) *J. Gen. Physiol.* **108,** 237–250
61. Choe, H., Sackin, H., and Palmer, L. G. (1998) *J. Gen. Physiol.* **112,** 433–446
62. Pardo, L. A., Heinemann, S. H., Terlau, H., Ludewig, U., Lorra, C., Pongs, O., and Stuhmer, W. (1992) *Proc. Natl. Acad. Sci. U. S. A.* **89,** 2466–2470
63. Ilan, N., Zilberberg, N., Gonzalez-Colaso, R., and Goldstein, S. A. N. (1999) *Biophys. J.* **76,** 411 (abstr.)
64. Maingret, F., Fosset, M., Lesage, F., Lazdunski, M., and Honore, E. (1999) *J. Biol. Chem.* **274,** 1381–1387